The Biological Effect of Different Doses of Gold Nanoparticles on the Liver of Female Rats: A Histological and Immunohistochemical Study

Original Article

Amira Adly Kassab[1], Khalid Ahmed Ahmed Moustafa[1], Mohamed Hassan Ragab[2] and Ayah Mohamed Hassan Ragab[3]

[1]Department of Histology and Cell Biology, [2]Department of Anatomy, Faculty of Medicine, Tanta University, Tanta, Egypt

[3] Department of Reproductive Health and Family Planning, National Research Centre, Giza, Egypt

ABSTRACT

Background: Gold nanoparticles [GNPs] are significant scientific achievements which are effectively employed in medicine. However, in vivo biological impact of these particles should be assessed to investigate their safety on human health.

Aim: Study of the biological effect of different gold nanoparticles doses on the liver of adult female rats exploring the novel mechanisms of gold nanoparticles induced liver damage.

Materials and Methods: Forty adult female rats were separated into one control group [Group I] and two GNPs-treated groups [Group II; 40µg/kg and Group III; 400µg/kg]. Specimens of the liver were taken to be processed for the light and electron microscopy in addition to immunohistochemical staining technique for the p53 protein, tumor necrosis factor alpha [TNF-α] and B-cell lymphoma 2 [Bcl-2].

Results: Administration of gold nanoparticles to adult female rats caused various histological deterioration in the liver depending on the dose. Hepatocytes showed vacuolated cytoplasm and pyknotic nuclei. Dilation and congestion of the central veins, blood sinusoids, hepatic artery and portal vein were seen. Disrupted endothelial layer was observed in some central veins. An apparent increase in kupffer cells and mononuclear cellular infiltration were observed. The immunohistochemical results demonstrated a significant increase in p53 and TNF-α and decrease in Bcl-2 immunoreactions. Ultrastructurally, swollen or damaged mitochondria, dilated rough endoplasmic reticulum [RER] and apparent glycogen depletion were observed in the hepatocytes.

Conclusion: Gold nanoparticles induced various dose dependent histological deterioration, inflammation and apoptosis in the liver of adult female rats. So, it should be given cautiously to females to avoid liver damage.

Received: 27 July 2020, **Accepted:** 28 August 2020

Key Words: Electron microscopy, GNPs, immunohistochemistry, liver.

Corresponding Author: Amira A. kassab, MD, Department of Histology and Cell Biology, Faculty of Medicine, Tanta University, Egypt, **Tel.**: +20 10 16697635, **E-mail:** Amirakassab80@yahoo.com

ISSN: 1110-0559, Vol. 44, No.2

INTRODUCTION

Nanotechnology is effectively implemented in diverse fields that employ nanoparticles (NPs) in many medical devices and food industries[1]. Nowadays, the application of NPs as a diagnostic or therapeutic method has proved success[2]. Nanoparticles are mainly used for gene delivery, cancer treatment, photothermal therapy and imaging techniques[3,4]. The effective medical possibility of NPs was attributed to their chemical stability, biocompatibility and ease of synthesis[5]. They are effectively employed in the release of peptides[6], antibiotics[7], amino acids[8], anticancer drugs[9], antioxidants[10], glucose[11], nucleic acids[12] and isotopes[13].

The physicochemical NPs characters result in a marked reactivity with various tissues. So, despite of their significant useful applications, they may have serious health hazards[14]. Nanoparticles can damage the biological membranes and can be accumulated in diverse organs as liver, spleen and kidney[15,16]. There are different reports about in vivo bad impact of these particles[17,18]. The undesired impacts are correlated to their size which is a main factor for reactive oxygen species {ROS} synthesis[2].

Gold nanoparticles (GNPs) have assorted routes to get in the body as skin touch, ingestion and inhalation[19]. The oral one possessed a highest toxicity in experimental rats[20]. They are characterized by wide systemic distribution that is inversely correlated with their sizes[21,22]. The smaller particles offered wide systemic distribution to brain, kidney, lungs, liver, heart, spleen, thymus and reproductive organs[23,24]. GNPs can also damage genes leading to inflammation and cell death[25,26].

 DOI: 10.21608/ejh.2020.37340.1335

The balance between the successful medical potency and adverse effects of GNPs were not sufficiently tested[27]. Former studies tested the in vitro influence of GNPs. However, more in vivo biological studies are needed to test the wanted safety of GNPs[28,29,30].

Sex variations were formerly studied with other nanoparticles. It was found that the kidneys of female animals displayed a higher NPs concentration than the other sex group[31,32]. Although most researchers have focused on testing the impact of GNPs on liver of male animals[33], their influence on females should be tested due to their vulnerability.

Therefore, this research purposed to study the biological effect of different gold nanoparticles doses on the liver of female rats exploring the novel mechanisms of GNPs induced liver injury by utilizing assorted histological techniques.

MATERIALS AND METHODS

Chemicals

Gold Nanospheres: Turkevich protocol was used for GNPs preparation through the standard citrate reduction to give mono-disperse spherical GNPs {10–15 nm in diameter[34,35].

Study design

The animal work followed the guidelines for animal use of the Ethics Committee for Scientific Research of the National Research Center, Egypt. Forty adult female albino rats {140-160 grams} were available in the experiment. They were subjected to a standard 12-h light/12-h dark cycle in suitable cages with proper ventilation before and throughout the work. They had free access to a balanced laboratory diet as well as water ad libitum.

The rats were arranged into

1. Group I (control group): 20 rats were subdivided into 2 equal subgroups: the first (subgroup IA) received no treatment and the second (subgroup IB) received 1 ml distilled water orally daily for 14 days.
2. Group II (low dose group): 10 rats received 40µg gold nanoparticles/kg {in 1ml distilled water} orally daily for 14 days[36].
3. Group III (high dose group): 10 rats received 400µg gold nanoparticles/kg {in 1ml distilled water} orally daily for 14 days[36].

At the end of the experiment, rats were anesthetized by giving intraperitoneal pentobarbital injection {40 mg/kg}[37]. The liver was rapidly dissected and specimens from the right lobe were handled for light and electron microscopy.

Light microscopic study

Liver specimens were fixed in neutral buffered formalin {10%}, washed, dehydrated in ascending grades of ethanol, cleared in xylol and embedded in paraffin. Then, liver sections {5µm thickness} were stained with haematoxylin and eosin [H&E] to study the histological features[38].

For immunohistochemical staining, liver sections (5µm thickness) were dewaxed, rehydrated, and washed with phosphate buffered saline {PBS}. The liver sections were incubated with the following primary antibodies: (rabbit polyclonal antibody against p53 protein, ab131442, Abcam, Cambridge, USA, 1:100 dilution); (rabbit polyclonal antibody against tumor necrosis factor-alpha (TNF-α), ab6671, Abcam, 1/100 dilution); (rabbit polyclonal antibody against B-cell lymphoma2 (Bcl-2), Abcam, ab59348, at a dilution of 1/100) overnight in a humid chamber at 4°C and then incubated for 60 minutes with biotinylated goat anti-rabbit IgG at room temperature. Sections were incubated with a streptavidin–biotin–horseradish peroxidase complex for another 60 minutes. The immunoreactivity was visualized by 3,3′-diaminobenzidine (DAB) hydrogen peroxide (a chromogen). Sections were also counterstained with Mayer's haematoxylin. The negative control sections of the liver were prepared without using any of the mentioned primary antibodies[39]. Positive control for p53 was human breast carcinoma. Positive control for TNF-α was human tonsil. Positive control for Bcl-2 was human colon carcinoma. The liver cells with brown nuclei were p53-immunopositive cells. The liver cells with brown cytoplasm were TNF-α and Bcl-2 immunopositive cells.

For transmission electron microscope, specimens of the liver were processed according to the commonly used routine protocol. They were embedded in epoxy resin mixture. Ultrathin sections (80-90nm) were stained with uranyl acetate as well as lead citrate[40]. JEOL-JEM-100 transmission electron microscope was employed to check the grids {at Electron Microscopic Unit of Tanta University}.

Morphometric study

Immunohistochemical evaluation occurred by employing an image analysis system {Leica Q (500), MC program} at Central Research Lab. at Tanta Faculty of Medicine, Tanta University. Ten non-overlapping fields were examined in each slide for area percentage {area %} of the positive reaction of p53 (X1000), TNF-α and Bcl-2 (X400) {in DAB-stained sections}.

Statistical analysis

The area percentage (%) of p53, TNF- α and Bcl-2 immunoreactions were subjected to one-way analysis of variance {ANOVA} as well as Tukey's procedure. Statistical package for social sciences statistical analysis software {SPSS Inc., version 11.5, USA} was utilized. The mean values as well as the standard deviation values {Mean ± SD} for all groups were calculated. Probability values {*P values*} < 0.05 and < 0.001 were significant and highly significant values respectively[41].

RESULTS

No deaths were observed and there was zero mortality index in all groups during this study.

1-H&E results

Group I (control group): All subgroups showed the

same features of the liver parenchyma. The sections showed branching cords of hepatocytes that radiated from a central vein. The hepatocyte cords were separated by the blood sinusoids which were lined by endothelial cells as well as Kupffer cells. The polyhedral hepatocytes had granular acidophilic cytoplasm and most of them had large rounded vesicular nuclei with prominent nucleoli while some were binucleated (Figure 1). There were portal areas containing connective tissue stroma, branches of the portal vein and bile duct (Figure 2).

Group II (low dose group): The examination revealed some structural changes in a few areas in the liver. These were in the form of dilated congested central veins and vacuolated hepatocytes. Some vacuolated cells showed rounded vesicular nuclei, while others showed shrunken deeply stained nuclei (Figures 3,4). Other hepatocytes appeared with homogenous acidophilic cytoplasm and vesicular nuclei with mononuclear cellular infiltration near the congested central vein (Figure 5). Another observation was the apparent increase in kupffer cell number (Figures 3,5). Regarding the portal areas dilated congested branch of the portal vein, dilated branches of the hepatic artery and mononuclear cellular infiltration were noticed (Figure 6).

Group III (high dose group): Severe hepatic structural changes were detected in this group. Markedly dilated and congested central veins and blood sinusoids were seen with disrupted endothelial layer of some central veins (Figures 7,8,9). Moreover, many hepatocytes appeared with markedly vacuolated cytoplasm and contained shrunken deeply stained nuclei (Figure 10). Some hepatocytes showed homogenous acidophilic cytoplasm and vesicular nuclei with mononuclear cellular infiltration near the congested central vein. There was also an apparent increase in Kupffer cells (Figure 11). The portal areas showed dilated congested branches of the portal vein and hepatic artery with mononuclear cellular infiltration (Figure 12).

2-Immunohistochemical results

P53 immnunostaining: p53-immunostained liver sections of Group I (control group) displayed a weak positive brown nuclear reaction in a few hepatocytes (Figure 13). In Group II (low dose group), a moderate positive nuclear reaction for p53 was detected in some cells (Figure 14), while in Group III (high dose group), a strong positive nuclear immunoreaction for p53 was observed in many cells (Figure 15).

TNF-α immunostaining: Immunostained liver sections of Group I (control group) exhibited an extremely weak positive brown immunoreaction to TNF-α (Figure 16), while sections from Group II (low dose group) expressed a moderate positive brown immunoreaction in the cytoplasm of some hepatocytes (Figure 17). Moreover, sections of Group III (high dose group) expressed a strong positive reaction in many hepatocytes (Figure 18).

Bcl-2 immunostaining: Immunostained liver sections of Group I (control group) displayed a strong positive reaction to Bcl-2 in the form of brown coloration of the cytoplasm of many hepatocytes (Figure 19), while sections from Group II (low dose group) expressed a moderate positive immunoreaction in many hepatocytes (Figure 20). Moreover, sections of Group III (high dose group) expressed a weak positive reaction to Bcl-2 in many hepatocytes (Figure 21).

3-Electron microscopic results

Ultrastructurally, examination of Group I (control group) revealed polyhedral hepatocytes containing rounded euchromatic nuclei with prominent nucleoli. The cytoplasm contained numerous mitochondria that appeared variable in size as well as in shape. The mitochondria were associated with rough endoplasmic reticulum (RER). Rosettes of glycogen granules were observed in the cytoplasm (Figure 22).

In Group II (low dose group), the ultrastructural examination revealed a few hepatocytes with irregular shrunken nuclei, peripheral heterochromatin and vacuolated cytoplasm (Figure 23). On the other hand, a few hepatocytes showed swollen distorted mitochondria, dilated smooth endoplasmic reticulum, dilated RER and perinuclear space. Small lipid droplets appeared in the cytoplasm. (Figures 24,25).

Group III (high dose group) showed severe ultrastructural changes affecting many hepatocytes. Markedly vacuolated cytoplasm with apparent glycogen depletion was observed in many hepatocytes. Many irregular shrunken heterochromatic nuclei were observed (Figures 26,27). Numerous swollen disrupted mitochondria were noticed with destroyed cristae which were associated with dilated RER and perinuclear space (Figures 28,29). The gold nanoparticles were clearly seen in the cytoplasm (Figure 26).

4-Morphometric & statistical results (Table 1)

The area percentage {area %} of p53 immunoreaction of hepatocytes displayed a significant elevation in Group II compared to Group I. Moreover, Group III possessed a highly significant elevation compared to Group I.

The area % of TNF-α immunoreaction of hepatocytes in Group II expressed a significant rise compared to Group I. Moreover, Group III displayed a highly significant rise compared to Group I.

The area % of Bcl-2 expression of hepatocytes in Group II displayed a significant reduction compared to Group I. Moreover, Group III showed a highly significant reduction compared to Group I.

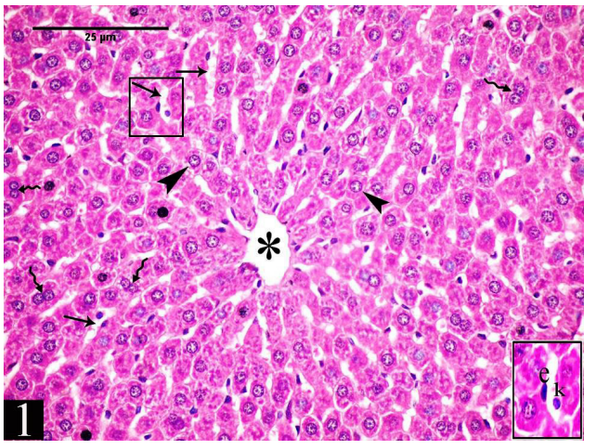

Fig. 1: A photomicrograph showing the normal hepatic architecture with a central vein (*) and cords of hepatocytes (arrow head) having granular cytoplasm and large rounded vesicular nuclei and separated by the blood sinusoids (arrow). Notice the binucleated hepatocytes (wavy arrow). The inset shows the lining endothelium (e) and kupffer cells (k) of the blood sinusoids (Group I, H&E X 400, Inset X1000).

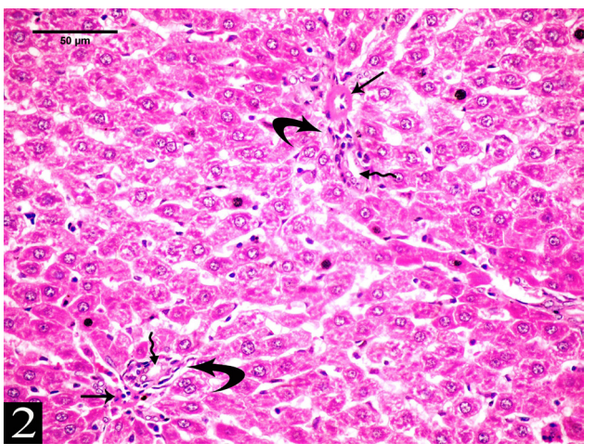

Fig. 2: showing the portal areas (curved arrow), branches of the portal vein (arrow) and bile duct (wavy arrow). (Group I, H&E X 400).

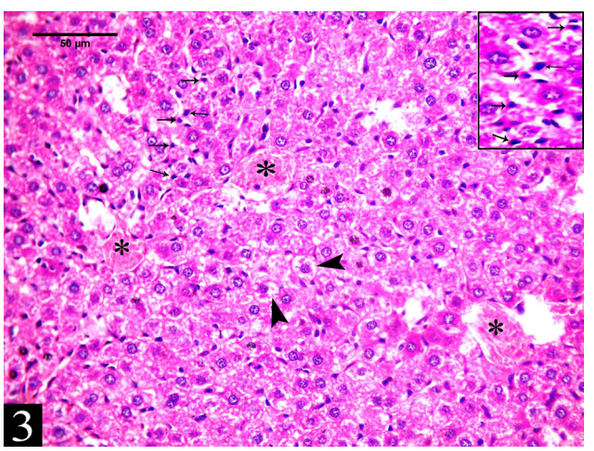

Fig. 3: showing dilated congested central veins (*) and vacuolated hepatocytes with rounded vesicular nuclei (arrow head). The inset shows an apparent increase in kupffer cells (arrow) (Group II, H&E X 400, Inset X1000).

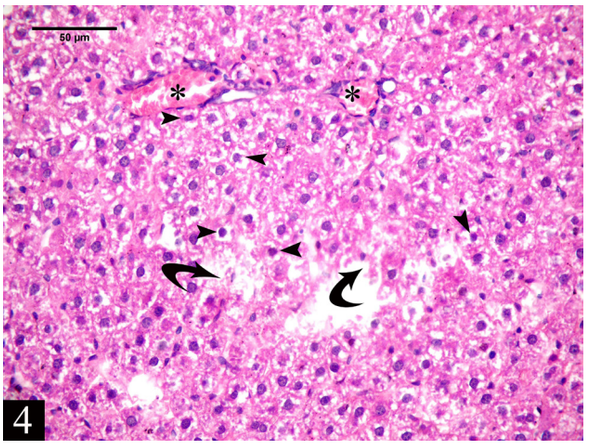

Fig. 4: showing congested central veins (*) and vacuolated hepatocytes with shrunken deeply stained nuclei (arrow head). Notice a few destroyed cells (curved arrow). (Group II, H&E X 400).

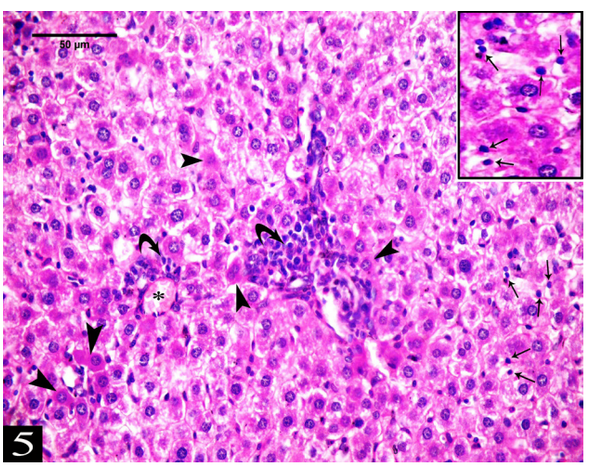

Fig. 5: showing some hepatocytes with homogenous acidophilic cytoplasm and vesicular nuclei (arrow head) with mononuclear cellular infiltration (curved arrow) near the congested central vein (*). The inset shows an apparent increase in kupffer cells (arrow) (Group II, H&E X 400, Inset X1000).

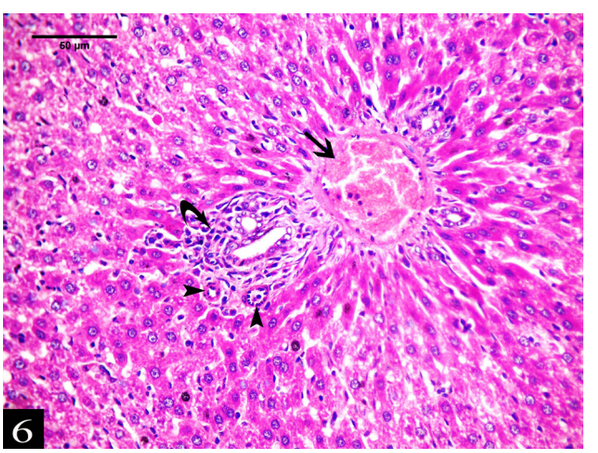

Fig. 6: showing a dilated congested branch of the portal vein (arrow), dilated branches of the hepatic artery (arrow head) and mononuclear cellular infiltration (curved arrow). (Group II, H&E X 400).

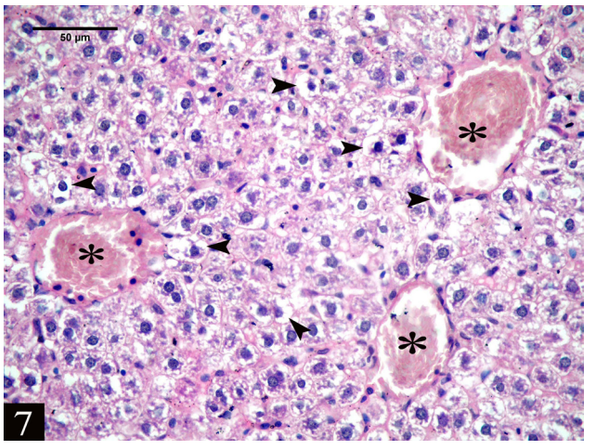

Fig. 7: showing markedly dilated and congested central veins (*) and marked cytoplasmic vacuoles of the surrounding hepatocytes (arrow head). (Group III, H&E X 400).

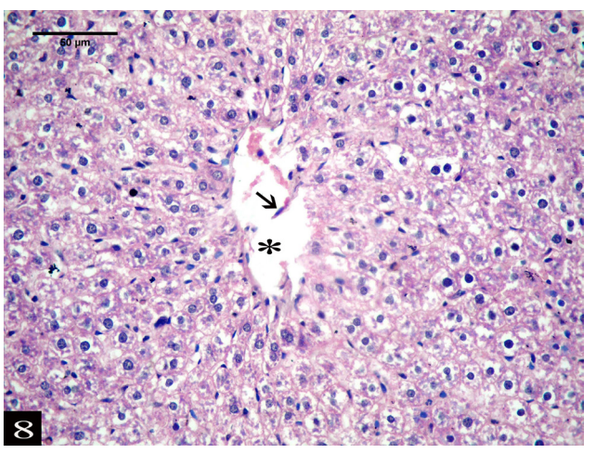

Fig. 8: showing disrupted endothelial layer (arrow) of a central vein (*). (Group III, H&E X 400).

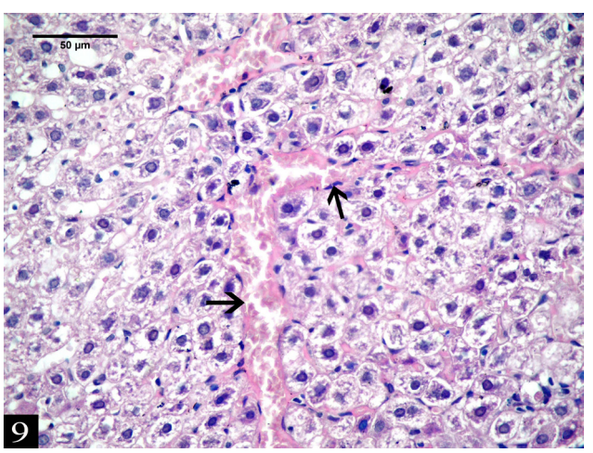

Fig. 9: showing markedly dilated and congested blood sinusoids (arrow). (Group III, H&E X 400).

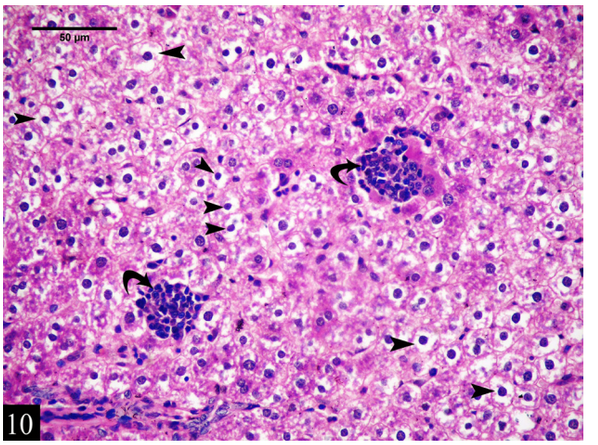

Fig. 10: showing hepatocytes with markedly vacuolated cytoplasm and shrunken deeply stained nuclei (arrow head) and mononuclear cellular infiltration (curved arrow). (Group III, H&E X 400).

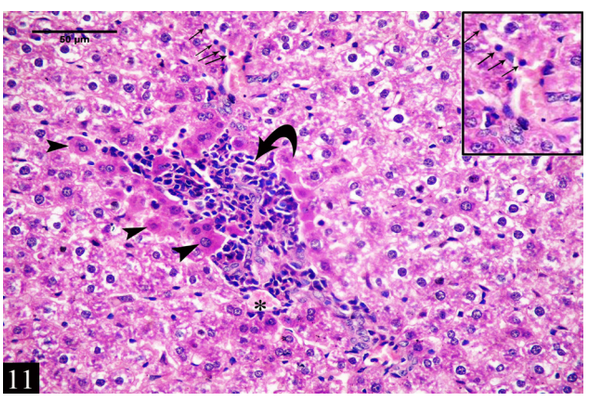

Fig. 11: showing hepatocytes having homogenous acidophilic cytoplasm and vesicular nuclei (arrow head) with mononuclear cellular infiltration (curved arrow) near the congested central vein (*).The inset shows an apparent increase in kupffer cells (arrow). (Group III, H&E X 400, Inset X1000).

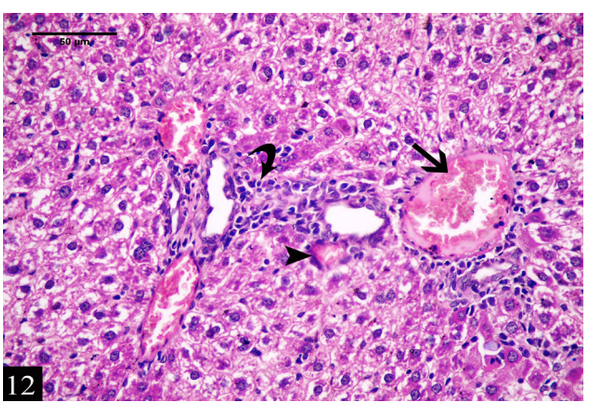

Fig. 12: showing dilated congested branches of the portal vein (arrow) and hepatic artery (arrow head) with mononuclear cellular infiltration (curved arrow). (Group III, H&E X 400).

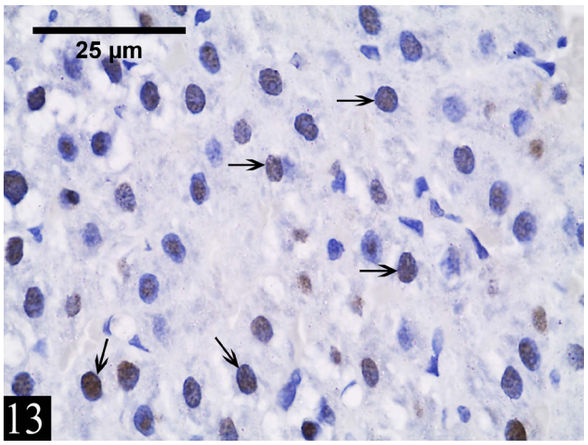

Fig. 13: showing a weak positive brown nuclear immunoreaction for p53 (arrow) in a few hepatocytes. (Group I, p53-immunostaining, X1000).

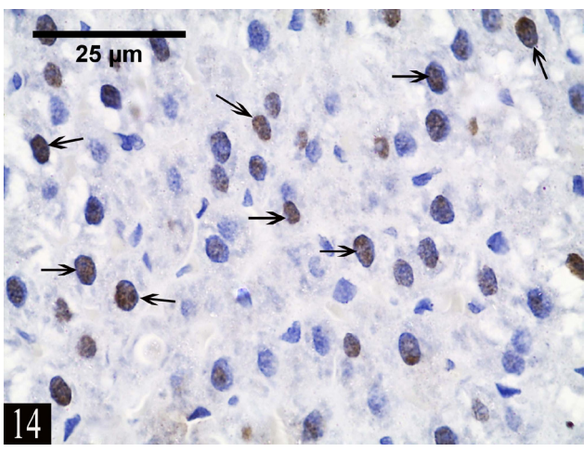

Fig. 14: showing a moderate positive nuclear p53 immunoreaction (arrow) in some hepatocytes. (Group II, p53-immunostaining, X1000).

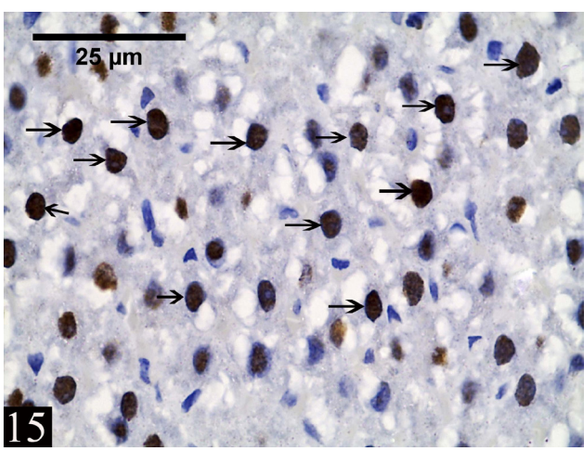

Fig. 15: showing a strong positive nuclear immunoreaction for p53 (arrow) in many hepatocytes. (Group III, p53-immunostaining, X1000).

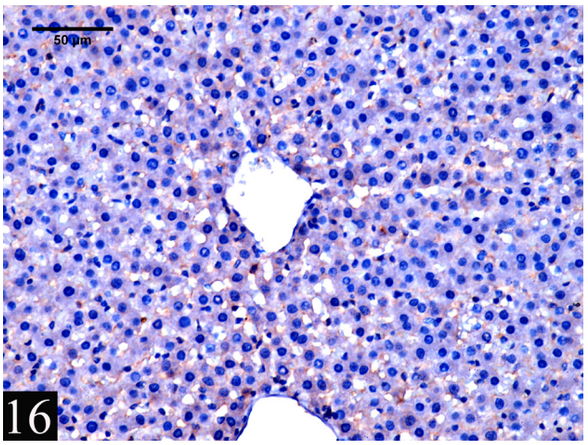

Fig. 16: showing an extremely weak positive brown immunoreaction to TNF-alpha. (Group I, TNF-alpha immunostaining, X400).

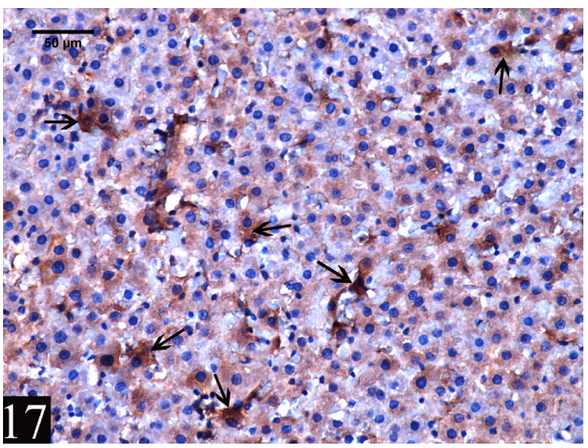

Fig. 17: showing a moderate positive immunoreaction to TNF-alpha (brown coloration) in the cytoplasm of some hepatocytes (arrow). (Group II, TNF-alpha immunostaining, X400).

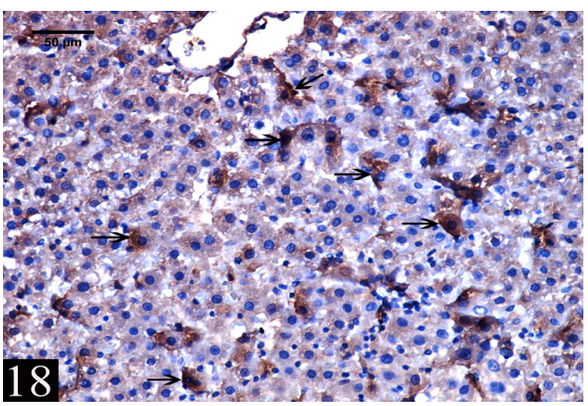

Fig. 18: showing a strong positive immunoreaction to TNF-alpha in the cytoplasm of many hepatocytes (arrow). (Group III, TNF-alpha immunostaining, X400)

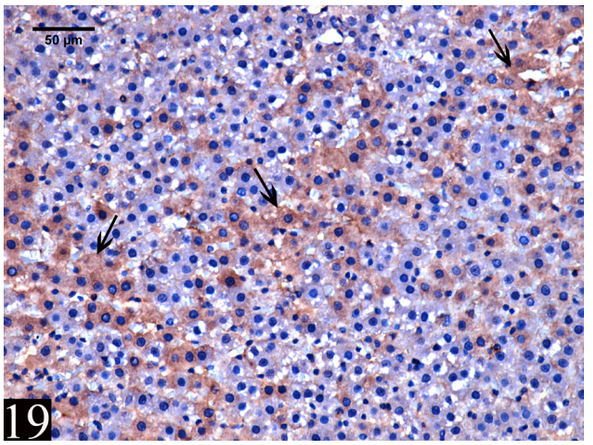

Fig. 19: showing a strong positive immunoreaction to Bcl-2 (brown coloration) in the cytoplasm of many hepatocytes (arrow). (Group I, Bcl-2 immunostaining, X400)

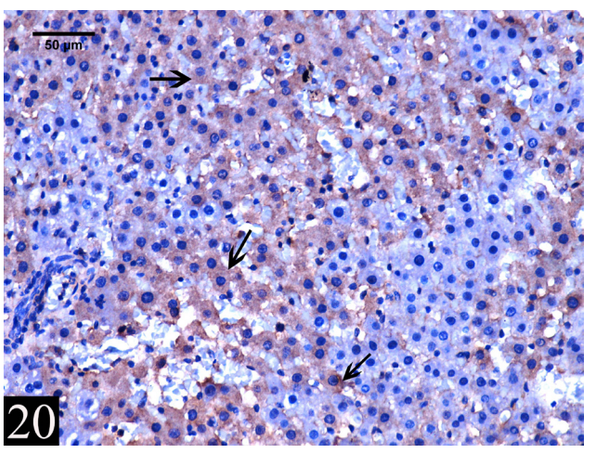

Fig. 20: showing a moderate positive immunoreaction to Bcl-2 in the cytoplasm of many hepatocytes (arrow). (Group II, Bcl-2 immunostaining, X400).

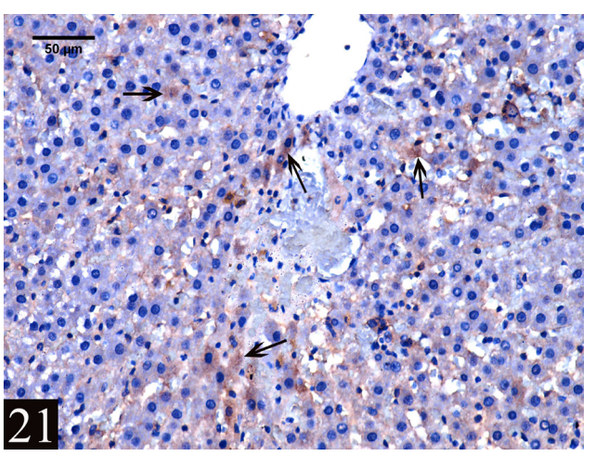

Fig. 21: showing a weak positive immunoreaction to Bcl-2 in the cytoplasm of many hepatocytes (arrow). (Group III, Bcl-2 immunostaining, X400)

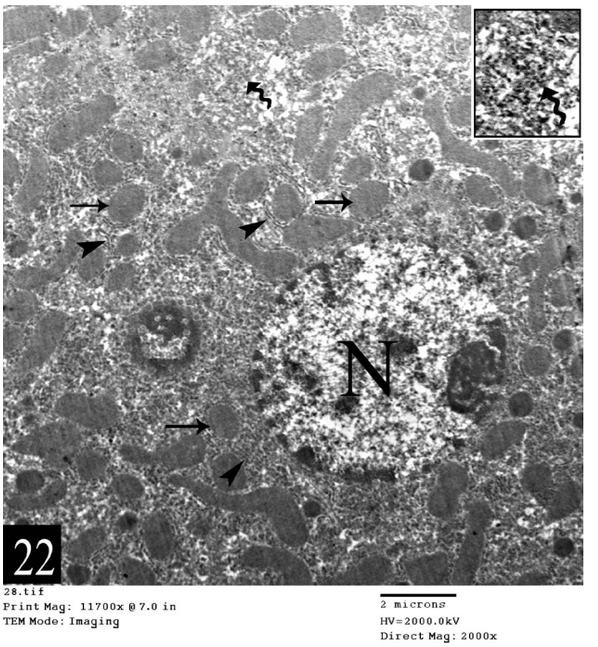

Fig. 22: An electron micrograph of a hepatocyte showing euchromatic nucleus (N), numerous mitochondria (arrow), rough endoplasmic reticulum (arrow head) and rosettes of glycogen granules (wavy arrow). (Group I, X 11700)

Fig. 23: An electron micrograph of a hepatocyte showing irregular shrunken nucleus having peripheral heterochromatin (N), vacuolated cytoplasm (curved arrow) and swollen mitochondria (arrow). (Group II, X 11700)

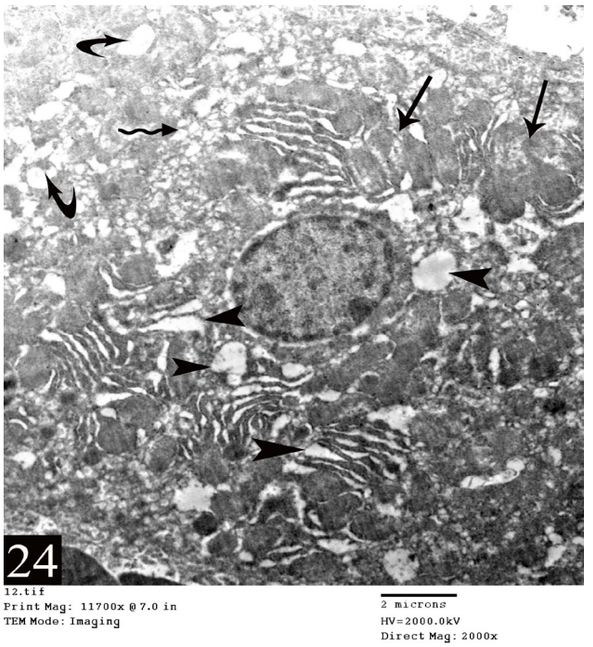

Fig. 24: An electron micrograph of a hepatocyte showing swollen distorted mitochondria (arrow), dilated smooth endoplasmic reticulum (wavy arrow) and dilated RER (arrow head). Notice the small cytoplasmic vacuoles (curved arrow). (Group II, X 11700)

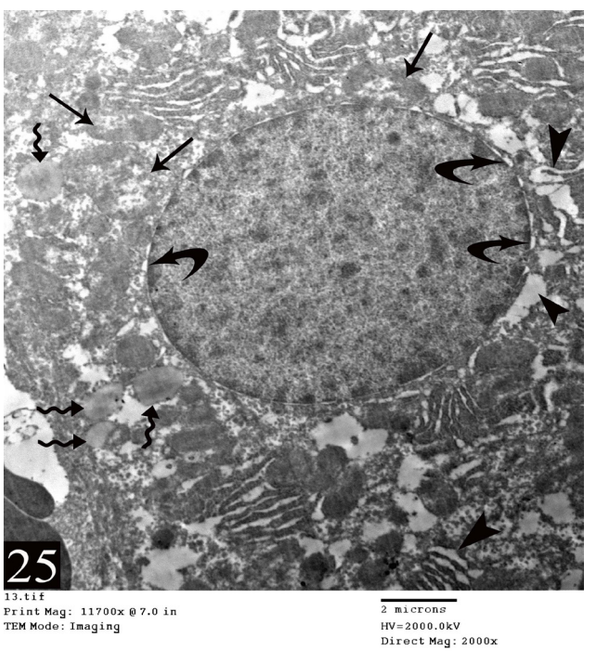

Fig. 25: An electron micrograph of a hepatocyte showing small lipid droplets (wavy arrow) and swollen mitochondria having destroyed cristae (arrow). Notice the dilated RER (arrow head) and perinuclear space (curved arrow). (Group II, X 11700)

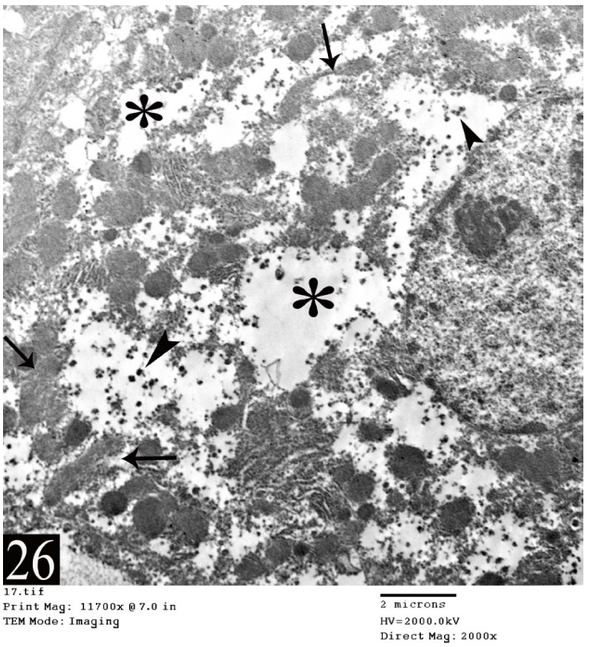

Fig. 26: An electron micrograph of a hepatocyte showing markedly vacuolated cytoplasm with apparent glycogen depletion (*) and destroyed mitochondria (arrow). Notice the intracellular gold nanoparticles (arrow head). (Group III, X 11700)

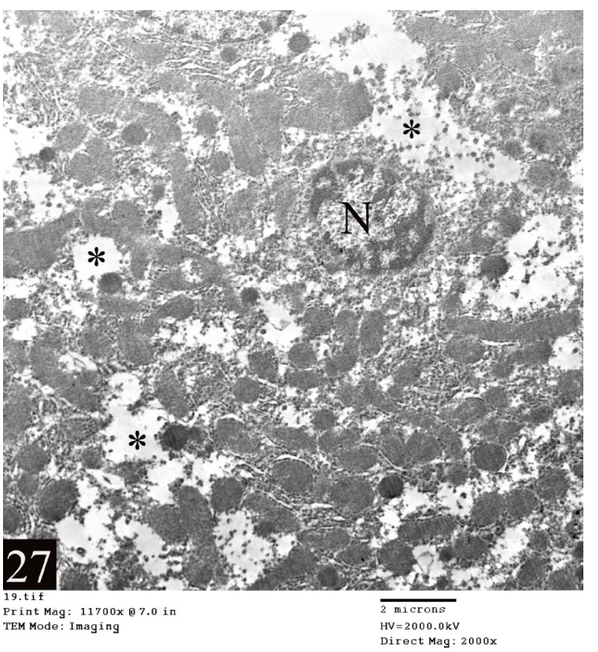

Fig. 27: An electron micrograph of a hepatocyte showing irregular shrunken nucleus with peripheral heterochromatin (N). Notice the markedly vacuolated cytoplasm (*). (Group III, X11700)

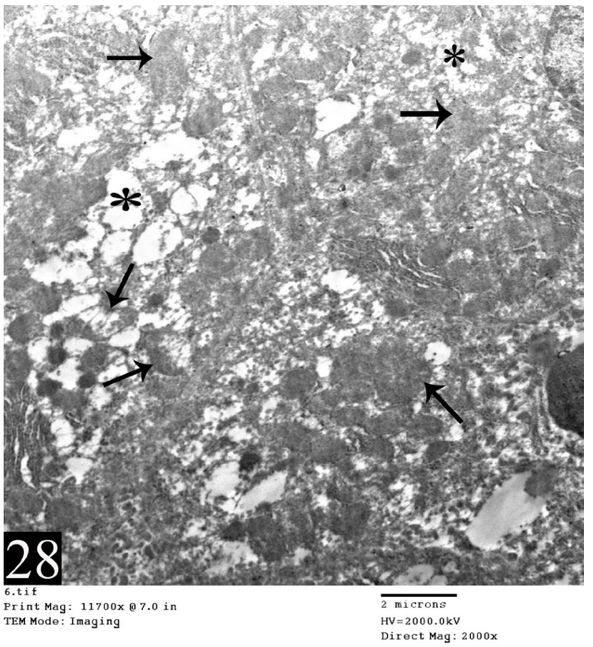

Fig. 28: An electron micrograph of parts of three hepatocytes showing swollen mitochondria with destroyed cristae (arrow) and marked cytoplasmic vacuoles (*). (Group III, X 11700)

Fig. 29: An electron micrograph of a hepatocyte showing markedly dilated RER (arrow head) and perinuclear space (curved arrow). (Group III, X 11700)

Table 1: illustrates area % {Mean ± SD} of p53, TNF-α and Bcl-2 immunoreactions

Parameters \ Groups	Group I (control group)	Group II (low dose group)	Group III (high dose group)
Mean area % of p53	3.283±0.122	3.477±0.225*	5.998±0.400**
Mean area % of TNF-α	8.934±0.510	11.16±2.01*	16.59±1.80**
Mean area % of Bcl-2	27.738±0.833	26.623±0.707*	19.967±0.925**

*P < 0.05 and **P< 0.001 are significant and highly significant values versus

DISCUSSION

Gold nanoparticles are successfully applied for medical diagnosis and various treatment protocols such as tumor diagnosis and cancer therapy as well as targeted and effective delivery of many drugs[3,4]. Their biological toxicity to male animals had been investigated in many research works[33,42]. Females are a vulnerable group because nanoparticles could influence their reproductive activity as well as the fetal development[43]. So, their influence on female animals should be investigated. Therefore, this work purposed to investigate the biological effects of different gold nanoparticles doses on the liver of female rats exploring novel mechanisms of GNPs induced liver injury.

In this study, histological evaluation of liver sections obtained from GNPs treated female rats revealed significant morphological changes such as vacuolated cytoplasm and pyknotic nuclei of hepatocytes, dilation and congestion of the central veins, blood sinusoids, hepatic artery and portal vein. Disrupted endothelial layer was observed in some central veins. An apparent increase in kupffer cells and mononuclear cellular infiltration were also found. The immunohistochemical results displayed a significant and/or a highly significant elevation in p53 and TNF-α and reduction in Bcl-2 immunoreactions. Ultrastructurally, swollen mitochondria, dilated RER and apparent glycogen depletion were observed. These findings were supported by other researchers who stated that liver damage could be caused by GNPs induced oxidative stress. Reactive oxygen species reacts with DNA resulting in DNA damage and apoptosis[44,45,46].

Gold nanoparticles induced liver damage might also arise from vacu¬olar degeneration as well as necrosis resulting from ROS. It was reported that GNPs exposure could induce inflammation, lipid change and vein intima disruption. Moreover, they could cause enhanced absorption of water by hepatocytes and vacuolization in addition to chronic inflammatory damage and fibrosis[47].

In our study, the liver cells showed cytoplasmic vacuolation which was interpreted by being as a cloudy swelling and indicates an acute liver injury. This was attributed to cell membrane damage by these particles causing water and Na+ influx. This results in cellular swelling, lysosomal damage and cytoplasmic degeneration. This finding may be also attributed to fatty changes which results from lipid peroxidation and organelle damage with detachment of the cytoplasmic lipoprotein[48].

One of the observed finding was appearance of liver cells with highly homogenous acidophilic cytoplasm. This is an initial sign of the hepatic necrotic changes before dissolution of the cell nucleus. This was attributed to mitochondria and endoplasmic reticulum swelling in addition to damage of lysosomes due to oxidative stress on the liver cells through glutathione depletion[49].

Another observation was a prominent and an apparent increase in the number of the Kupffer cells. GNPs activate the phagocytic activity of these cells to remove nanoparticles. This finding may be a defense mechanism of detoxification and may contribute to hepatic oxidative stress[50]. Moreover, it may be considered as a compensatory response in order to clear cellular debris. These cells can also stimulate the immune cells to get rid of any foreign substances and also to help in the regeneration[51].

Moreover, GNPs induced nuclear changes mainly pyknosis and nuclear irregularity. It is considered as a sign for cell death and denotes a liver injury associated with protein metabolism disturbances[17,48].

Inflammatory cellular infiltration of the hepatic tissue and congestion of the blood vessels were seen in the present study and may be due to the interaction of GNPs with the hepatic interstitial tissue. This interferes with the antioxidant defense mechanisms initiating the inflammatory response. Moreover, there was also disruption of the endothelial layer of some central veins that was caused by endothelial cell damage and vascular stress induced by GNPs[48].

Ultrastructurally, the study showed that GNPs exerted variable deleterious effects on the hepatocyte structure in the form of degeneration and swelling of the mitochondria and RER in addition to the nuclear changes. GNPs-induced oxidative stress may result in mitochondrial dysfunctions as a decline of ATP synthesis and an increased ROS. So, mitochondrial affection could disturb the cellular metabolism and affect cell viability inducing apoptosis and necrosis[52]. Moreover, GNPs caused endoplasmic reticulum swelling which is attributed to loss of protein synthesis and the liver detoxification function. Endoplasmic reticulum change is considered an early indicator for GNPs toxicity[53]. GNPs can also reach the nucleus and affect the genetic material leading to destruction of their morphology and damage of DNA[54]. Glycogen depletion upon GNPs exposure was a prominent finding and was attributed to oxidative stress induced by the nanoparticles on hepatocytes[55,56].

The immunohistochemical study displayed a significant dose-dependent elevation in TNF-α expression in GNPs treated rats. TNF-α is a pro-inflammatory cytokine and its up regulation denotes an inflammation mediated by GNPs exposure. TNF-α plays an essential role in the inflammatory processes in addition to its immunomodulatory functions. Moreover, the oral intake of these nanoparticles causes their interaction with the gut wall lymphocytes or macrophages which are moved out with their immune products to other body tissues[57]. In addition, production of cytokines is being a natural immunological defense activity to any foreign particles. However, if these cytokines act effectively for long time, it will generate excessive ROS with more cellular injury[58].

P53 protein is a tumor suppressor protein that acts as a nuclear transcription factor to activate genes of apoptosis. P53 plays a pro-apoptotic role because it can initiate apoptosis when DNA damage happens. Therefore, the significant elevation in p53 nuclear expression upon GNPs administration could suggest DNA damage and this may be the mechanism of GNPs induced liver injury. p53 protein can be also transferred to the mitochondria liberating other pro-apoptotic agents as Fas and Bax. In addition, our results revealed also a significant reduction in Bcl-2 expression upon GNPs administration. Bcl-2 is an anti-apoptotic protein that prevents the mitochondrial liberation of the pro-apoptotic agents inhibiting apoptosis. The reduced Bcl-2 expression was attributed to the increase in the expression of p53 or to ROS accumulation and activation of the oxidizing enzymes by the nanoparticles leading to mitochondrial damage and cell death. So, the modulation of the expression of these apoptotic associated proteins p53 and Bcl-2 in the present study may explain the possible mechanisms involved in GNPs induced liver injury[59,60].

CONCLUSION AND RECOMMENDATIONS

This study revealed that GNPs caused dose dependent histological deterioration, and various degrees of inflammation and apoptosis in the liver of female rats. The study also suggests the possible participation of TNF-α, p53 and Bcl-2 in the development of GNPs induced liver damage. So, high doses of GNPs should be avoided. Moreover, GNPs should be given cautiously to females as they are a particular vulnerable group. Further clinical studies on human are also needed to confirm the results of the animal studies.

CONFLICT OF INTERESTS

There are no Conflicts of interest.

REFERENCES

1. Cai W, Gao T, Hong H, Sun J. Application of Au nanoparticles in cancer nanotechnology. Nanotech Sci Appl. 2008; 1: 17-32.

2. Abdelhalim MAK, Qaid HAY, Al-Mohy YH, Ghannam MM. The Protective Roles of Vitamin E and α-Lipoic Acid Against Nephrotoxicity, Lipid Peroxidation, and Inflammatory Damage Induced by Gold Nanoparticles. International Journal of Nanomedicine 2020; 15: 729-734.

3. Masse F, Ouellette M, Lamoureux G, Boisselier E. Gold nanoparticles in ophthalmology. Med Res Rev. 2019; 39(1): 302-327.
4. Yahyaei B, Nouri M, Bakherad S, Hassani M, Pourali P. Effects of biologically produced gold nanoparticles: toxicity assessment in different rat organs after intraperitoneal injection. AMB Expr 2019; 9(38): 1-12.
5. Panchapakesan B, Book-Newell B, Sethu P, Rao M, Irudayaraj J. Gold nanoprobes for theranostics. Nanomedicine (Lond). 2011; 6(10): 1787-1811.
6. Bastús NG, Sánchez-Tilló E, Pujals S, Farrera C, Kogan MJ, Giralt E, Celada A, Lloberas J, Puntes V. Peptides conjugated to gold nanoparticles induce macrophage activation. Mol Immunol. 2009; 46(4): 743-748.
7. Tom RT, Suryanarayanan V, Reddy PG, Baskaran S, Pradeep T. Ciprofloxacin-protected gold nanoparticles. Langmuir 2004; 20(5): 1909–1914.
8. Ipe BI, Mahima S, Thomas KG. Light-induced modulation of self-assembly on spiropyran-capped gold nanoparticles: a potential system for the controlled release of amino acid derivatives. J Am Chem Soc. 2003; 125(24): 7174-7175.
9. Craig GE, Brown SD, Lamprou DA, Graham D, Wheate NJ. Cisplatin-tethered gold nanoparticles that exhibit enhanced reproducibility, drug loading, and stability: a step closer to pharmaceutical approval? Inorganic Chemistry 2012; 51(6): 3490–3497.
10. Simpson CA, Salleng K J, Cliffel DE, Feldheim DL. In vivo toxicity, biodistribution, and clearance of glutathionecoated gold nanoparticles. Nanomedicine 2013; 9(2): 257–263.
11. Song K, Xu P, Meng Y, Geng F, Li J, Li Z, Xing J, Chen J, Kong B. Smart gold nanoparticles enhance killing effect on cancer cells. Int J Oncol. 2013; 42(2): 597-608.
12. Ghosh R, Singh LC, Shohet JM, Gunaratne PH. A gold nanoparticle platform for the delivery of functional microRNAs into cancer cells. Biomaterials 2013; 34(3): 807–816.
13. Guerrero S, Herance JR, Rojas S, Mena JF, Gispert JD, Acosta GA, Albericio F, Kogan MJ. Synthesis and in vivo evaluation of the biodistribution of a 18F-labeled conjugate gold-nanoparticle-peptide with potential biomedical application. Bioconjug Chem. 2012; 23(3): 399-408.
14. Adewale OB, Davids H, Cairncross L, Roux S. Toxicological behavior of gold nanoparticles on various models: influence of physicochemical properties and other factors. International Journal of Toxicology 2019; 38(5): 357-384.
15. De Jong WH, Burger MC, Verheijen MA, Geertsma RE. Detection of the presence of gold nanoparticles in organs by transmission electron microscopy. Materials 2010; 3: 4681-4694.
16. Babadi VY, Najafi L, Najafi A, Gholami H, Zarji ME, Golzadeh J, Amraie E, Shirband A. Evaluation of iron oxide nanoparticles effects on tissue and enzymes of liver in rats. J Pharm Biomed Sci. 2012; 23(23): 1-5.
17. Abdelhalim MAK and Moussa SAA. The gold nanoparticle size and exposure duration effect on the liver and kidney function of rats: in vivo. Saudi J Biol Sci. 2013 ;20:177–181
18. Pourali P, Badiee SH, Manafi S, Noorani T, Rezaei A, Yahyaei B. Biosynthesis of gold nanoparticles by two bacterial and fungal strains, Bacillus cereus and Fusarium oxysporum, and assessment and comparison of their nanotoxicity in vitro by direct and indirect assays. Electron J Biotechnol. 2017; 29: 86-93.
19. Buzea C, Pacheco II, Robbie K. Nanomaterials and nanoparticles:sources and toxicity. Biointerphases 2007; 2(4): 17-71.
20. Zhang X., Wu H., Wu D., Wang Y., Chang J., Zhai Z. Toxicological effects of gold nanoparticles in vivo by different administration routes. Int. J. Nanomed. 2010; 5: 771-781.
21. Sonavane G, Tomada K, Makino K. Biodistribution of colloidal gold nanoparticles after intravenous administration: effect of particle size. Colloids Surf B Biointerfaces. 2008; 66(2): 274-280.
22. Lasagna-Reeves C, Gonzalez-Romero D, Barria MA, Olmedo I, Clos A, Sadagopa Ramanujam VM, Urayama A, Vergara L, Kogan MJ, Soto C. Bioaccumulation and toxicity of gold nanoparticles after repeated administration in mice. Biochem Biophys Res Commun. 2010 ; 393(4): 649-655.
23. Khan HA, Abdelhalim MAK, Al-Ayed MS, Alhomida AS. Effect of gold nanoparticles on glutathione and malondialdehyde levels in liver, lung and heart of rats. Saudi J. Bio. Sci. 2012; 19: 461- 464.
24. Parveen A, Malashetty VB, Mantripragada B, Yalagatti MS, Abbaraju V, Deshpande R. Bio-functionalized gold nanoparticles: Benign effect in Sprague-Dawley rats by intravenous administration. Saudi J Biol Sci. 2017; 24(8): 1925-1932.
25. Wim H., De Jong, Werner I. Particle size–dependent organ distribution of gold nanoparticles after intravenous administration. Biomaterials. 2008; 29: 1912-1919.
26. Cho WS, Cho MJ, Jeong J , *ET AL*. Acute toxicity and pharmacokinetics of 13 nm-sized PEG-coated gold nanoparticles. Toxicol Appl Pharmacol. 2009; 236(1): 16-24.
27. Carneiro H, Barbosa MF, Fernando. Gold nanoparticles. a critical review of therapeutic applications and toxicological aspects. J. Toxicol. Environ. Health, Part B. 2016; 19: 129-148.

28. Gu Q, Cuevas E, Ali SF, Paule MG, Krauthamer V, Jones Y, Zhang Y. An alternative in vitro method for examining nanoparticle-induced cytotoxixity. International Journal of Toxicology 2019; 38(5): 385-394.
29. Raghunandan D, Ravishankar B, Sharanbasava G. Anti–cancer studies of noble metal nanoparticles synthesized using different plant extracts. Cancer Nano. 2011; 2: 57-65.
30. Parveen A and Rao S. Cytotoxicity and genotoxicity of biosynthesized gold and silver nanoparticles on human cancer cell lines. J. Clust. Sci. 2015; 26: 775-788.
31. Heydrnejad MS and Samani RJ. Sex Differential Influence of Acute Orally-administered Silver nanoparticles (Ag-NPs) on Some Biochemical Parameters in Kidney of Mice Mus musculus. J Nanomed Nanotechnol. 2016; 7(3): 1000382.
32. Kim WY, Kim J, Park JD, Ryu HY, Yu IJ. Histological study of gender differences in accumulation of silver nanoparticles in kidneys of Fischer 344 rats. J Toxicol Environ Health A. 2009; 72(21-22) : 1279-1284.
33. Doudi M and Setorki M. The acute liver injury in rat caused by gold nanoparticles. Nanomed J. 2014; 1(4): 248-257.
34. Turkevich J, Stevenson PC, Hillier J. A study of the nucleation and growth processes in depends the synthesis of colloidal gold. Discuss Faraday Soc. 1951; 11: 55-75.
35. Zabetakis K, Ghann WE, Kumar S, Daniel MC. Effect of high gold nanoparticles prepared by an extended Turkevich- Frens method. Gold Bull, 2012; 45(4): 203-211.
36. Okasha EF and Ragab AMH. Histological, immunohistochemical and ultrastructural study on the effect of gold nanoparticles on the left ventricular cardiac myocytes of adult male albino rat. Middle East J. Sci. Res. 2015; 23(12): 2968-2982.
37. Gaertner DJ, Hallman TM, Hankenson FC, Batcherder MA. Anesthesia and analgesia for laboratory rodents. Anesthesia and analgesia in laboratory animals. 2nd edition. Academic press, San Diego, CA. Boston. 2008; 239 -240.
38. Bancroft JD and Gamble M. Theory and practice of histological techniques. 6th ed. Philadelphia: Churchill Livingstone: Elsevier Health Science. 2008; 126–127.
39. Ramos-Vara JA, Kiupel M, Baszler T, Bliven L, Brodersen B, Chelack B, Czub S, Del Piero F, Dial S, Ehrhart EJ, Graham T, Manning L, Paulsen D, Valli VE, West K. Suggested guidelines for immunohistochemical techniques in veterinary diagnostic laboratories. J Vet Diagn Invest. 2008; 20: 393–413.
40. Bozzola JJ and Russell LD. Electron microscopy: principles and techniques for biologists, second edition, Boston, Jones and Bartlett Publishers 1999; 100-124.
41. Dawson-Saunders B and Trapp R. Basic and clinical biostatics. 3rd ed., Lang Medical Book, McGrow Hill Medical Publishing Division. 2001; 161-218.
42. Hassan ZA, Obaid HH, Al-Darraji MN. The toxicity of gold nanoparticles on liver function of albino mice. International Journal of Advanced Science and Technology 2020; 29(9s): 542-548.
43. Sun J, Zhang Q, Wang Z, Yan B. Effects of nanotoxicity on female reproductivity and fetal development in animal models. Int J Mol Sci. 2013; 14(5): 9319-9337.
44. Abdelhalim MAK, Moussa SAA, Qaid HAY. The protective role of quercetin and arginine on gold nanoparticles induced hepatotoxicity in rats. International Journal of Nanomedicine 2018; 13: 2821-2825.
45. Patlolla AK, Kumari SA, Tchounwou PB. A comparison of poly-ethylene-glycol-coated and uncoated gold nanoparticle-mediated hepatotoxicity and oxidative stress in Sprague Dawley rats. International Journal of Nanomedicine 2019; 14: 639-647.
46. Ferreira GK, Cardoso E, Vuolo FS, Michels M, Zanoni ET, Carvalho-Silva M, Gomes LM, Dal-Pizzol F, Rezin GT, Streck EL, Paula MM. Gold nanoparticles alter parameters of oxidative stress and energy metabolism in organs of adult rats. Biochemistry and cell biology 2015; 93(6): 548-557.
47. Abdelhalim MAK, Moussa SAA, Qaid HAY, Al-Ayed MS. Potential effects of different natural antioxidants on inflammatory damage and oxidative-mediated hepatotoxicity induced by gold nanoparticles. International Journal of Nanomedicine 2018; 13: 7931–7938.
48. Abdelhalim M A and Jarrar B M. Gold nanoparticles administration induced prominent inflammatory, central vein intima disruption, fatty change and Kupffer cells hyperplasia. Lipids in health and disease 2011; 10: 133.
49. Pandey G, Srivastava DN, Madhuri S. A standard hepatotoxic model produced by paracetamol in rat. Toxicology international 2008; 15(1): 69-70.
50. Neyrinck A. Modulation of Kupffer cell activity: phsio-pathological consequences on hepatic metabolism. Bull Mem Acad R Med Belg. 2004; 159(5-6): 358-66.
51. Almansour MI and Jarrar BM. Protective effect of propolis against pulmonary histological alterations induced by 10 nm naked gold nanoparticles. Chiang Mai J. Sci. 2017; 44(2): 449-461.
52. Maurer LL and Meyer JN. A systematic review of evidence for silver nanoparticle-induced mitochondrial toxicity. Environ Sci Nano. 2016; 3(2): 311-322.
53. He C, Jiang S, Yao H, *et al*. Endoplasmic reticulum stress mediates inflammatory response triggered by ultra-small superparamagnetic iron oxide nanoparticles in hepatocytes. Nanotoxicology. 2018;12 (10):1198–1214.

54. Yao Y, Zang Y, Qu J, Tang M, Zhang T. The toxicity of metallic nanoparticles on liver: The subcellular damages, mechanisms, and outcomes. International Journal of Nanomedicine 2019;14: 8787–8804.

55. Almansour MI, Alferah MA, Shraideh ZA, Jarrar BM. Zinc oxide nanoparticles hepatotoxicity: Histological and histochemical study. Environ Toxicol Pharmacol. 2017; 51: 124-130.

56. Almansour M, Sajti L, Melhim W, Jarrar BM. Ultrastructural hepatocytic alterations induced by silver nanoparticle toxicity. Ultrastruct Pathol. 2016; 40(2): 92-100.

57. Elsabahy E and Wooley KL. Cytokines as biomarkers of nanoparticle immunotoxicity. Chem Soc Rev. 2013; 42(12): 5552–5576.

58. Khan HA, Ibrahim KE, Khan A, Alrokayan SH, Alhomida AS. Immunostaining of proinflammatory cytokines in renal cortex and medulla of rats exposed to gold nanoparticles. Histol Histopathol. 2017; 32: 597-607.

59. Banu H, Renuka N, Faheem SM, Ismail R, Singh V, Saadatmand Z, Khan SS, Narayanan K, Raheem A, Prenkumar K, Vasanthakumar G. Gold and silver nanoparticles biomimetically synthesized using date palm pollen extract-induce apoptosis and regulate p53 and Bcl-2 expression in human breast adenocarcinoma cells. Biological Trace Element Research 2018; 186: 122-134.

60. El-Azab NE and El-Mahalaway AM. A histological and immunohistochemical study on testicular changes induced by silver nanoparticles in adult rats and the possible protective role of camel milk. Egyptian Journal of Histology 2019; 42(4): 1044-1058.

الملخص العربى

التأثير البيولوجى للجرعات المختلفة لجسيمات الذهب النانوية على كبد إناث الجرذان: دراسة هستولوجية و هستوكيميائية مناعية

أميرة عدلى كساب[١]، خالد أحمد أحمد مصطفى[١]، محمد حسن رجب[٢]، آية محمد حسن رجب[٣]

[١]قسم الهستولوجيا وبيولوجيا الخلايا, كلية الطب,جامعة طنطا,مصر

[٢]قسم التشريح ,كلية الطب,جامعة طنطا,مصر

[٣]قسم الصحة الإنجابية وتنظيم الأسرة,المركز القومى للبحوث,الجيزة,مصر

المقدمة: تعتبر جسيمات الذهب النانوية من الإنجازات العلمية الهامة التي تم توظيفها بنجاح في الطب. ومع ذلك, يجب تقييم التأثير البيولوجي لهذه الجسيمات فى الجسم الحى للتحقق من سلامتهم على صحة الإنسان.

الهدف من البحث: دراسة التأثير البيولوجى للجرعات المختلفة لجسيمات الذهب النانوية على كبد إناث الجرذان وإستكشاف آليات جديدة مسببة لتلف الكبد الناجم عن جسيمات الذهب النانوية.

مواد وطرق البحث: تم تقسييم أربعين من إناث الجرذان البالغة إلى مجموعة واحدة ضابطة (المجموعة الأولى) ومجموعتين معالجتين بجسيمات الذهب النانوية (المجموعة الثانية ؛ ٤٠ ميكروجرام / كجم والمجموعة الثالثة ؛ ٤٠٠ ميكروجرام / كجم). تم أخذ عينات الكبد وتجهيزها للمجهر الضوئى والإلكترونى بالإضافة إلى تقنية صبغات هستوكيميائية مناعية لبرتين ب ٥٣ (p٥٣) وبروتين عامل نخر الورم ألفا (TNF-α) و بروتين ورم الغدد الليمفاوية٢ (٢-Bcl).

النتائج: إعطاء جسيمات الذهب النانوية لإناث الجرذان البالغة سبب تدهور نسيجي فى الكبد حسب الجرعة. أظهرت الخلايا الكبدية فجوات فى السيتوبلازم وأنوية صغيرة وداكنة. شوهد تمدد واحتقان الأوردة المركزية ، والجيوب الدموية ،و الشريان الكبدي والوريد البابي. ولوحظ تقطع فى الطبقة المبطنة لبعض الأوردة المركزية. كما لوحظ زيادة واضحة في خلايا كوبفر وتسلل خلوي أحادي النواة. وقد أظهرت الدراسة الهستوكيميائية المناعية زيادة ذات دلالة إحصائية في التفاعل المناعى ل p٥٣ و TNF-α وإنخفاض في Bcl-٢. وعلى مستوى التركيب الدقيق فقد لوحظ تورم أوتلف الميتوكوندريا وإتساع الشبكة الإندوبلازمية الخشنة وإستنزاف الجليكوجين.

الإستنتاج: جسيمات الذهب النانوية سببت تدهور نسيجى معتمدة على الجرعة و إلتهاب وموت الخلايا المبرمج فى كبد إناث الجرذان. لذا، يجب إعطاؤه بحذر للإناث لتجنب تلف الكبد.